

Kinetic studies on the formation of silver nanoparticles by reduction of silver(I) with glucose in aqueous and micellar media

H.A. Ewais^{1*}, I.M. Ismail^{1,2}, K.H. Al-Fahami¹

¹Chemistry Department, Faculty of Science, King Abdulaziz University, P.O. Box 80203, Jeddah 21413, Saudi Arabia.

²Center of Excellence in Environmental Studies, King Abdulaziz University, P.O. Box 80216, Jeddah 21589, Saudi Arabia

Received January 7, 2016; Revised April 14, 2017

The kinetics of the formation of silver nanoparticles (AgNPs) by reduction of silver (I) with glucose are studied at different temperatures in aqueous micellar media. The reaction was carried out under pseudo-first-order condition by taking the [glucose] (>10-fold) the [Ag⁺]. The effect of [NaOH], [Ag⁺], [glucose] and [CTAB] are investigated. Rate of reaction enhance by increasing [OH⁻]. CTAB stabilized the rate of growth of nanoparticles and the rate of reaction increases with increasing in temperature. It was observed that nanoparticles are spherical, aggregated and poly dispersed. On the basis of kinetic data, a suitable mechanism is proposed and discussed for the silver sol formation. The particle size of silver sols is characterized by the transmission electron microscopic (TEM) and some physicochemical and spectroscopic tools.

Keywords: Silver nanoparticles; kinetics and mechanism; micelles; reduction; TEM

INTRODUCTION

Metal nanoparticles are attractive due to their easy synthesis, modification as well as their size, shape, distribution which are properties dependent [1, 2]. The preparation of uniform nanosized drug particles with specific size, shape and chemical properties is of great interest in the formulation of new pharmaceutical products [3,4]. Nanoparticles can be used as labels for optical bio-detection, substrate for multiplexed aqueous bioassays, probes for cellular imaging or carriers for therapeutic delivery [5]. The evolution and technological progress of silver nanoparticles in the manufacture are due to their antiviral and antibacterial properties, in addition to numerous industrial applications including microelectronics, cosmetics, an adhesives and catalysis to enhanced solar cells [6-8]. The formation of nanoparticles using biological entities has great important due to their individual shape dependent optical, electrical and chemical properties have potential application in biotechnology [1].

The nanoparticles were formed and stabilized by chemical and physical methods; the chemical method, such as, electrochemical techniques, chemical reduction, and photochemical reduction is most widely used [9] and [10]. The chemical reduction is the most used method for the formation of silver nanoparticles as stable, colloidal dispersions in aqueous or non-aqueous media [11] and [12]. Hydrazine, aniline, ascorbic acid, lactose

and sodium borohydride are used as reducing agent in the formation of nanoparticles [13-17]. The stabilizing agent such as cetyltrimethylammonium bromide, sodiumdodecyl sulphate, Tritron X-100 and poly(vinyl alcohol) are used as capping agent to control the shape and size of silver nanocrystals [13,16,18]. The reduction of silver ions (Ag⁺) in aqueous medium gave a colloidal silver with particle diameters of several nanometers [19]. The oligomeric clusters of nanosilver are formed by reducing of Ag⁺ to silver atoms (Ag⁰) [20]. The yellow colour of silver sols, which contain smaller particles, gave a peak in the wavelength range 390-450 nm [20].

In this paper, the kinetics of formation of silver nanoparticles by reduction method were studied in order to obtain a stable, narrow size, uniform and spherical shape form of silver nanoparticle in aqueous micellar media. Also, the role of [OH⁻] in the silver sols formation is investigated.

EXPERIMENTAL

Materials and solutions

Silver nitrate, glucose, cetyltrimethylammonium bromide, sodium hydroxide and potassium permanganate (BDH Ltd Poolle England) were used without further purification. The solutions of silver nitrate and glucose were prepared daily (to arrest the aerial oxidation) in cooled and boiled water. Doubly distilled water was used for the preparation of all solutions.

* To whom all correspondence should be sent:

E-mail: hshalby2002@yahoo.com

Kinetic procedures

UV–visible LABOMED, INC UVD-2960 spectrophotometer and Perkin Elmer EZ-150 recording spectrophotometer were used to monitor the absorbance of the formation of silver sols. TEM images for the determination of the size of silver particle were recorded using transmission electron microscope (JEOL, JEM-1011, Japan) The preparation of samples were carried out by adding a drop of working solution on a carbon-coated standard copper grid (300 mesh) operating at 80 kV. The particles were imaged by LEO 440i Scanning Electron Microscopy (SEM) at an accelerating voltage of 20 kV.

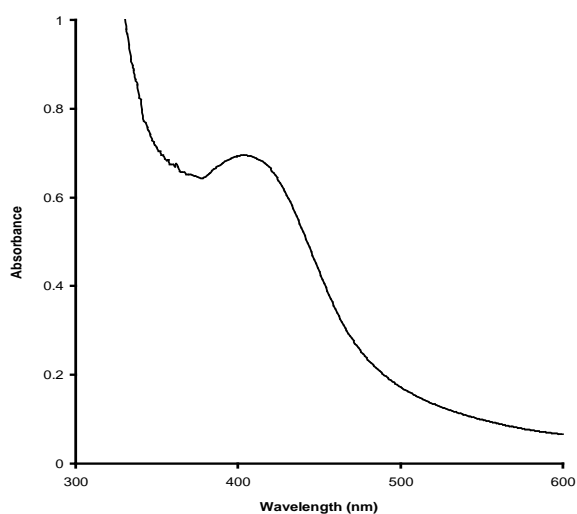


Fig. 1. Absorbance spectra of silver sol. Reaction conditions: $[Ag^+] = 5.0 \times 10^{-5} \text{ mol dm}^{-3}$, $[glucose] = 2.0 \times 10^{-3} \text{ mol dm}^{-3}$, $[CTAB] = 1.0 \times 10^{-3} \text{ mol dm}^{-3}$, $[OH^-] = 5.0 \times 10^{-3} \text{ mol dm}^{-3}$ and $T = 50 \text{ }^\circ\text{C}$.

The ultraviolet-visible absorption spectra of the products (silver sol) were followed spectrophotometrically for a definite period of time using the LABOMED, INC UVD-2960 spectrophotometer. All reactants were equilibrated at the required temperatures in a thermostated water bath for ca. 15 min before being thoroughly mixed and quickly transferred to an absorption cell. The reaction rates were measured by monitoring the absorbance of product at 405 nm, on a Perkin Elmer EZ-150 spectrophotometer, where the absorption of the products is maximal. The temperature of the reacting solution was adjusted, using automatic circulation thermostat. The thermostat was provided with a special pumping system for circulating water at regulated temperature in the cell holder.

Pseudo-first-order conditions were maintained in all runs by the presence of a large excess (>10-fold) of maltose. Pseudo-first-order rate constants, k_{obs} , were obtained from the slopes of plots of \ln

$a/(1-a)$ versus time with a fixed-time method where $a = A_t/A_\infty$ and A_t and A_∞ are the absorbencies at times t and infinity, respectively [21].

The preparation of silver nanoparticles by the reduction of silver (I) with glucose in presence of micelles in aqueous medium was investigated. A series of runs were carried out, using a different concentration of glucose, silver nitrate and CTAB to obtain a perfectly clear silver sol. In the similar procedure, 2.0 ml of a $0.001 \text{ mol dm}^{-3}$ solution of silver nitrate and 2.0 ml of a 0.1 mol dm^{-3} sodium hydroxide solution was mixed with 4.0 ml of a 0.01 mol dm^{-3} CTAB solution. The pale yellow color of the silver sol is formed, when 4.0 ml of a 0.02 mol dm^{-3} solution of glucose was added to the reaction mixture at the beginning of reaction. The total volume of the reaction mixture was always 40 ml. The presence of pale yellow color, this indicated that the formation of Ag-nanoparticles [22, 23].

RESULTS AND DISCUSSION

Formation and characterization of silver nanoparticles

The synthesis and formation of silver nanoparticles using glucose as reducing agent in presence of active surfactants such as CTAB is very important because the shape and size depend on the nature of stabilizers and reducing agent [24]. For the characterization of silver sol, in a typical experiment, Ag^+ ions ($5.0 \times 10^{-5} \text{ mol dm}^{-3}$), $[NaOH]$ ($5.0 \times 10^{-3} \text{ mol dm}^{-3}$), glucose ($2.0 \times 10^{-3} \text{ mol dm}^{-3}$) with the CTAB ($1.0 \times 10^{-3} \text{ mol dm}^{-3}$) were mixed at $50 \text{ }^\circ\text{C}$.

UV–visible absorption spectra have been perfectly sensitive to the formation of silver sol because silver nanoparticles show a absorption peak due to the surface plasmon excitation and spectra of the product recorded were at the wavelength ranged from 300 to 600 nm (Fig. 1). The maximum absorption was obtained at wavelength 405 nm showing the formation of Ag-nanoparticles. This indicate that the increase in absorbance at 405 nm with time. The absorption plasmon band with a λ_{max} at 405 nm is the characteristic of spherical or roughly spherical shape Ag-nanoparticles synthesis.

From SEM images it is observed that the particles had a relatively narrow size and a spherical shape. The size of silver nanoparticle is ranging from 10.0 to 45.0 nm and has a various shapes: sphere and irregular with broader size distribution (Fig. 2).

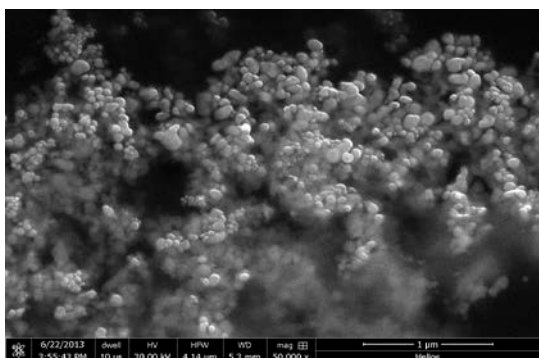


Fig. 2. SEM image of silver nanoparticle.

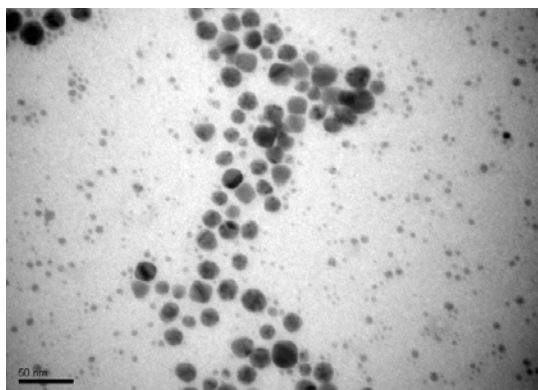


Fig. 3. TEM image of silver nanoparticle.

TEM image of the prepared Ag-nanoparticles is represented as shown in Fig. 3. From Fig. 3, it clear that the size of the nearly spherical nanoparticles ranges between 12.31 and 40.23 nm and their size distribution is relatively wide. The TEM image confirms that the CTAB stabilized particles are spherical rather than hexagonal forms of silver nanocrystals, as was observed for the reduction of Ag⁺ ions with hydrazine and ribose, respectively [25, 26].

Kinetics of formation of silver nanoparticles

Preliminary observations showed that the presence of NaOH solution is essential to the reduction of Ag⁺ ions by glucose in presence of CTAB. Therefore, the choice of the best conditions for the kinetic experiments is a crucial problem that we address first. In order to examine the effects of variables, experiments were tried at [Ag⁺] (1.25 – 6.25) × 10⁻⁵ mol dm⁻³, [glucose] (1.0 – 3.0) × 10⁻³ mol dm⁻³, [CTAB] (0.5–3.0) × 10⁻³ mol dm⁻³ and [NaOH] (2.50–15.0) × 10⁻³ mol dm⁻³.

Plotting absorbance versus time (Fig. 4) shows that non-catalytic and autocatalytic reaction path.

Table 1. Dependence of the [Ag⁺]/[glucose] reaction rate on [Ag⁺], [glucose] and [CTAB] = 1.0 x 10⁻³ mol dm⁻³ at T = 50.0 °C.

10 ³ [OH ⁻] mol dm ⁻³	10 ⁵ [Ag ⁺] mol dm ⁻³	10 ³ [glucose] mol dm ⁻³	10 ³ [CTAB] mol dm ⁻³	10 ³ k _{obs} s ⁻¹	
2.50	5.00	2.00	1.00	0.85	
3.75				1.36	
5.00				1.78	
7.50				3.46	
10.00				3.89	
12.50				4.03	
15.00				4.12	
5.00				5.00	1.00
5.00	1.50	1.12			
	2.00	1.78			
	2.50	2.32			
	3.00	2.73			
	2.00	1.60			
	2.50	1.51			
5.00	3.75	1.77			
	5.00	1.78			
	6.25	1.76			
	5.00	5.00	2.00	0.50	2.51
			0.75	2.03	
			1.00	1.78	
1.25			1.37		
			1.50	1.04	

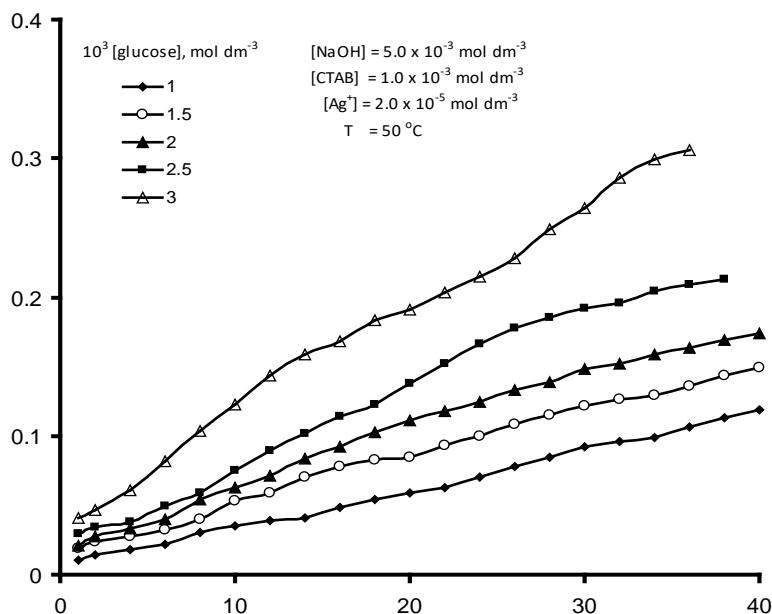


Fig. 4. Absorbance-time curves of silver sol formation at different [glucose]

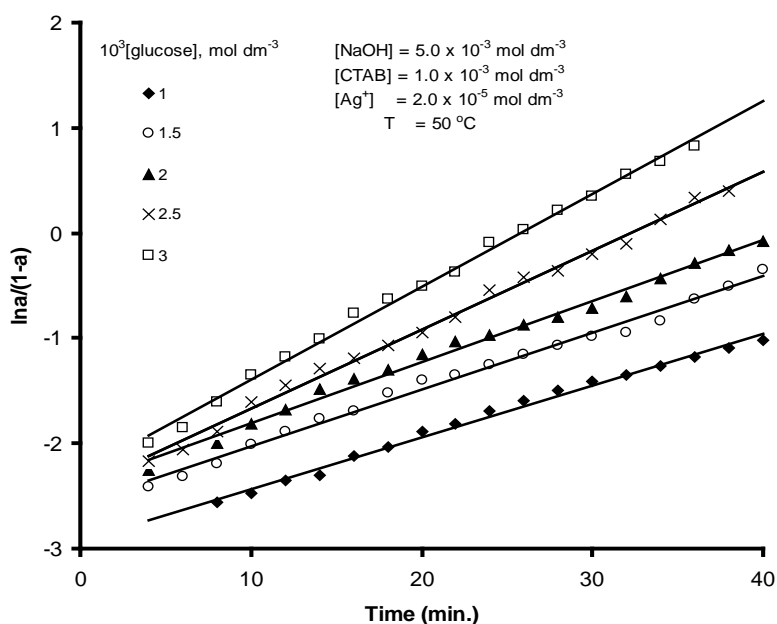


Fig. 5. Plots of $\ln a/(1-a)$ versus time at different [glucose] at 50 °C

The observation of autocatalysis in Fig. 4, is due to the formation of metal nucleation center which acts as a catalyst for the reduction of other silver ions present in solution. In the present study it is necessary to point out that the plots of $\ln a/(1-a)$ against time are linear up to > 87 % of the reaction (Fig. 5), where $a = A_t/A_\infty$ and A_t and A_∞ are the absorbancies at times t and infinity ∞ , respectively [21].

The values of the rate constants were obtained from the slopes of $\ln a/(1-a)$ versus time plots (Table 1).

The unaffected of k_{obs} over the $[Ag^+]$ range $(1.25-6.25) \times 10^{-5} \text{ mol dm}^{-3}$ at constant maltose concentration indicating first order dependence on the $[Ag^+]$ as shown in Table 1. The dependence of k_{obs} on glucose was examined over the concentration range $(1.0 - 3.0) \times 10^{-3} \text{ mol dm}^{-3}$ at fixed $[Ag^+]$, $[OH^-]$, CTAB and temperature. The kinetic data are graphically represented in Fig. 5. Table (1), shows that the rate constant, k_{obs} , increases with increasing in glucose concentration.

The kinetics of the formation of silver nanoparticles were carried out over a $[NaOH]$ range

of $(2.50 - 15.0) \times 10^{-3} \text{ mol dm}^{-3}$ at constant $[\text{R-CHO}] = 2.0 \times 10^{-3} \text{ mol dm}^{-3}$, $[\text{Ag}^+] = 5.0 \times 10^{-5} \text{ mol dm}^{-3}$, $[\text{CTAB}] = 1.0 \times 10^{-3} \text{ mol dm}^{-3}$ and at $T = 50 \text{ }^\circ\text{C}$. In absence of glucose, the solution become yellow transparent color and the spectra of this color were recorded as a function of time (Fig. 6). Fig. 6 shows that the spectra of $\text{Ag}^+ - \text{OH}^-$ reaction product cover the whole visible region of the spectrum in absence of glucose. No spectral peaks are observed for 40 min. Fig. 7 and Table 1, shows the dependency of k_{obs} on $[\text{NaOH}]$. The reaction is very sensitive to small concentration of NaOH, a

concentration of $2.5 \times 10^{-3} \text{ mol dm}^{-3}$ being enough to catalyses the reduction of Ag^+ by glucose. On the other hand, no reduction of Ag^+ ions takes place in absence of $[\text{OH}^-]$. The reaction rate increased with increasing $[\text{NaOH}]$ up to $7.5 \times 10^{-3} \text{ mol dm}^{-3}$ and no significant changes in k_{obs} were observed at $[\text{NaOH}] \geq 10.0 \times 10^{-3} \text{ mol dm}^{-3}$ (Fig. 7). These observations are in good agreement with the results of Huang et al. [27]. Thus we may safely conclude that hydroxide ions play a crucial role in the reaction of Ag^+ ions with paracetamol [27].

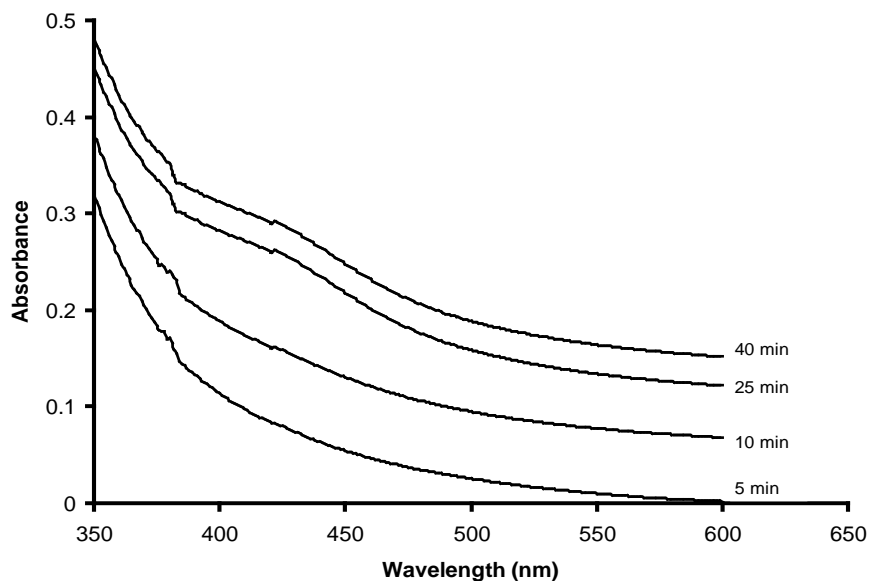


Fig. 6. Absorption spectra of silver sol formation as a function of time. Reaction conditions: $[\text{CTAB}] = 1.0 \times 10^{-3} \text{ mol dm}^{-3}$; $[\text{Ag}^+] = 5.0 \times 10^{-5} \text{ mol dm}^{-3}$; $[\text{NaOH}] = 5.0 \times 10^{-3} \text{ mol dm}^{-3}$; $T = 50 \text{ }^\circ\text{C}$

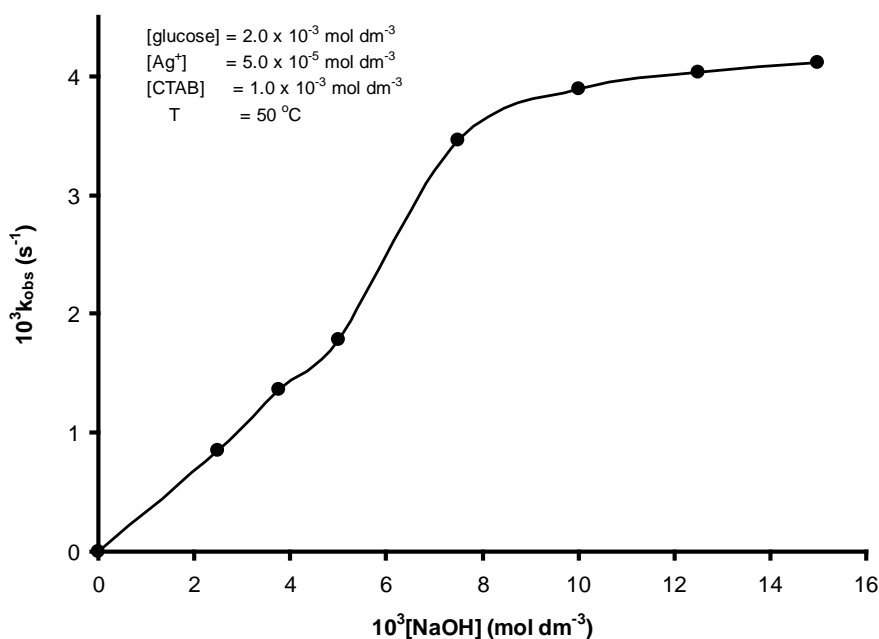


Fig. 7. Variation of k_{obs} with $[\text{NaOH}]$

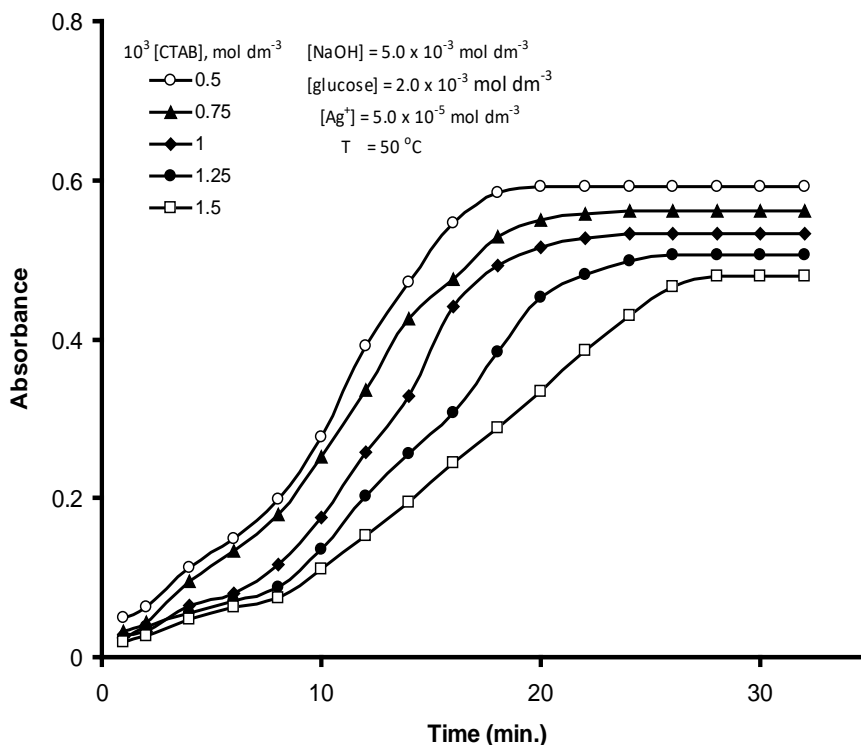


Fig. 8. Variation of absorbance versus time at different [CTAB].

Table 2. Variation of rate constant, k_{obs} , with temperatures.

Temp. (°C)	$10^3/T$ (K ⁻¹)	10^3k_{obs} (s ⁻¹)	$-\ln k_{obs}/T$ (s ⁻¹ K ⁻¹)
35.0	3.25	0.86	12.79
40.0	3.19	1.23	12.45
45.0	3.14	1.48	12.28
50.0	3.10	1.78	12.11
55.0	3.05	2.03	11.99

The effect of CTAB on the formation of silver nanoparticle by reduction with glucose was carried out at $[Ag^+] = 5.0 \times 10^{-5} \text{ mol dm}^{-3}$, $[glucose] = 2.0 \times 10^{-3} \text{ mol dm}^{-3}$, $[OH^-] = 5.0 \times 10^{-3} \text{ mol dm}^{-3}$ for a concentration range of CTAB = $(0.5 - 1.50) \times 10^{-3} \text{ mol dm}^{-3}$ and $T = 50.0 \text{ }^\circ\text{C}$. The kinetic data are graphically represented in Fig. 8. Table 1, indicates that the reaction rate decreases gradually with increasing of [CTAB].

The effect of temperature on the rate of reaction of glucose with silver ion was investigated at $[Ag^+] = 5.0 \times 10^{-5} \text{ mol dm}^{-3}$, $[glucose] = 2.0 \times 10^{-3} \text{ mol dm}^{-3}$, $[NaOH] = 5.0 \times 10^{-3} \text{ mol dm}^{-3}$ over the temperature range $(35.0 - 55.0) \text{ }^\circ\text{C}$. Variations of rate constant, k_{obs} , with different temperatures are represented in Table 2. show that the rate of reaction increases with increasing in temperatures (Table 2). From these results thermodynamic activation parameters including enthalpy and entropy associated with k_{obs} are obtained by plotting $-\ln k_{obs}/T$ against $1/T$, (c.f. Table 2. Enthalpy of

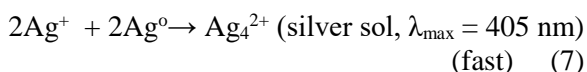
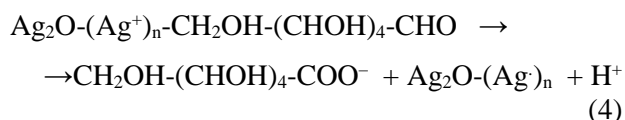
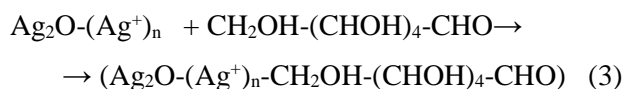
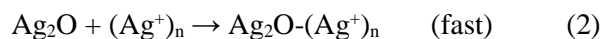
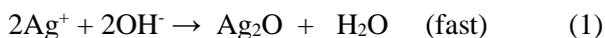
activation, ΔH^* and entropy of activation ΔS^* are equal to 33.1 kJ mol^{-1} and $-195.4 \text{ JK}^{-1}\text{mol}^{-1}$ respectively.

Mechanism

Before attempting to propose a mechanism for the silver sol formation, it is necessary to discuss on the species of Ag^+ existing in the NaOH medium. It is known that formation of silver particles in basic 2-propanol media proceed via formation of Ag_2O species involving the Ag^+ and OH^- [27, 28]. It should be emphasized here that the formation of transparent yellow color was also observed in a mixture of Ag^+ , CTAB and OH^- before the addition of glucose (Fig. 6). As the glucose is added, it results in a sudden increase in the absorbance. The Ag_2O is most probably in the colloidal form since no turbidity or precipitation is detected in the solution [27]. In order to identify the role of OH^- concentrations in the reduction Ag^+ ions by glucose, we experimentally tested that at specific

concentration of NaOH ($\geq 7.5 \times 10^{-3}$ mol dm⁻³), the reaction mixture ([CTAB] = 1.0×10^{-3} mol dm⁻³ and [Ag⁺] = 5.0×10^{-5} mol dm⁻³), turned turbid in absence of glucose. On the other hand, yellow transparent color appeared at lower [NaOH] ($\leq 7.5 \times 10^{-3}$ mol dm⁻³) and the spectra of this color was recorded as a function of time (Fig. 5), indicating the formation of colloidal Ag₂O during the fast reaction of Ag⁺ with OH⁻ [27]. These observations are in good agreement with the results of Huang et al. [27]. Thus we may safely conclude that hydroxide ions play a crucial role in the reaction of Ag⁺ ions with glucose. The hydroxide ions is known to have a catalytic effect on the formation of silver sols, provides the significant change in the reactivity of Ag⁺ ions that allow the initiation of the electron transfer from glucose to Ag⁺ ions, which in turn, preventing a fast corrosion of the very small silver particles at early stages of the reaction [27].

On the basis of these observations, the mechanism is proposed for the reduction of Ag⁺ by glucose. Eqs. (1) and (2) represents the fast formation of colloidal Ag₂O and adsorption of Ag⁺ from solution onto the surface of Ag₂O particles, respectively. The adsorption of organic reductants on the surface of the colloidal metal particles in quasi-equilibrium reactions prior to the redox rate-determining steps is widely accepted [29, 30]. Thus, the reaction proceeds through the adsorption of glucose onto the surface of colloidal Ag₂O–(Ag⁺)_n particles (Eq. (3)). By analogy with previous results, we assume that adsorbed silver ions are then reduced by reaction with glucose (Eq. (4); rate-determining step). In the next step, silver ions adsorbed on the surface of Ag₂O are then reduced via reaction with the delocalized electrons [29] (Eqs. (6) and (7)).



The role of micelles in catalysis and inhibition of some reactions are due to the solubilization

and/or incorporation of reactants into the small volume of micelles through electrostatic, hydrophobic, hydrogen bonding and Van der Waals forces [31, 32]. The role of CTAB in the formation of silver sols can be explained by the positive charge on Ag⁺ and its metal particles in the reaction medium. Furthermore, electrostatic repulsion between the positive head group (–N⁺(CH₃)₃) of CTAB micelles and Ag⁺ ions will explain why the rate of reaction decreases with increasing in [CTAB].

In comparison with the formation of silver nanoparticles by reduction with ribose [26] under the same condition, the rate-determining step path *via* one electron oxidation–reduction mechanism in both cases. The rate of formation of silver nanoparticles by the reduction with ribose is more than the rate of formation with glucose. The negative values of the entropies of activation for this reaction may result from the charge concentration of the reactants, which causes substantial mutual ordering of the solvated water molecules [33]. The intermolecular electron transfer steps are endothermic as indicated by the positive ΔH^* values. The support of ΔH^* and ΔS^* to the reaction rate seem to compensate each other. This suggests that the factors affecting ΔH^* should be closely related to those controlling ΔS^* .

CONCLUSIONS

The results from this study show that the reduction of silver (I) by glucose is enhanced in presence of NaOH, leading to the formation of stable and transparent yellow color of silver sol. The kinetics of silver sol formation was monitored by recording the absorbance as a function of time. The reaction proceeds through the adsorption of glucose onto the surface of colloidal Ag₂O–(Ag⁺)_n particles. TEM, SEM and UV-SP, show that the formation of spherical, aggregated and poly dispersed nanoparticles.

Acknowledgment: This project was funded by the Center of Excellence in Environmental Studies under grant number (1/W/1435-P/M). My thanks go the Ministry of Higher Education (MOHE) and Deanship of Scientific Research (DSR), King Abdulaziz University for the financial support.

REFERENCES

1. C. Burda, X. Chen, R. Narayanan, M.A. El-Sayed, *Chem. Rev.*, **105**, 1025 (2005).
2. J. Polte, *Cryst. Eng. Comm.*, **17**, 6809 (2015).
3. V.L. Colvin, *Nat. Biotechnol.*, **21**, 1166 (2003).

4. G. M. Sulaiman, E. H. Ali, I. I. Jabbar, A. H. Saleem, *Dig. J. Nanomater. Biost.*, **9**, 787 (2014).
5. A. Bansal, S.S. Verma, *Phys. Let. A*, **379**, 163 (2015)
6. V.K. Sharma, R.A. Yngard, Y. Lin, *Adv. Colloid Interface Sci.*, **145**, 83 (2009).
7. G.A. Sotiriou, S.E. Pratsinis, *Environ Sci Technol.*, **44**, 5649 (2010).
8. N.S. Wigginton, A. de Titta, F. Piccapietra, J. Dobias, V.J. Nesatyy, M.J.F. Suter, R. Bernier-Latmani, *Environ Sci Technol.*, **44**, 2163 (2010).
9. S. Irvani, H. Korbekandi, S.V. Mirmohammadi, B. Zolfaghari, *Res Pharm Sci.*, **9**, 385 (2014).
10. A. Frattini, N. Pellegrini, D. Nicastro, O. de Sanctis, *Mater Chem. Phys.*, **94**, 148 (2005)
11. K. M. Abou El-Nour, A. Eftaiha, A. Al-Warthan, R. A. Ammer, *Arab. J. Chem.*, **3**, 135 (2010).
12. M. Kiim, J.W. Byun, D.S. Shin, Y.S. Lee, *Mat Res Bull.*, **44**, 334 (2009).
13. I. M. Ismail, H. A. Ewais, *Oxid. Coummu.*, **39**, 62 (2016).
14. Z. Khan, S.A. Al-Thabati, A.Y. Obaid, A.O. Al-Youbi, *Colloids and Surf B: Biointerface*, **78**, 143 (2010).
15. J.A. Jacob, S. Kapoor, N. Biswas, T. Mukherjee, *Colloids Surf. A Physicochem. Eng. Aspects*, **301**, 329 (2007).
16. I. M. Ismail, H. A. Ewais, *Trans. Met. Chem.*, **40**, 371 (2015).
17. J. Polte, X. Tuaev, M. Wuthschick, A. Fischer, A. F. Thuenemann, K. Rademann, R. Kraehnert, F. Emmerling, *ACS Nano*, **6**, 5791 (2012).
18. A. Henglein, *Chem Mater*, **10**, 444 (1998.)
19. B. Wiley, Y. Sun, B. Mayers, *Chem. Eur. J.*, **11**, 454 (2005).
20. W. Qm, L. Ym, L. Kg, *Acc. Chem. Res.*, **48**, 1570 (2015).
21. K. Esumi, T. Hosoyo, A. Yamahira and K. Torigoe, *J Colloid Interface Sci.*, **226**, 346 (2000).
22. V.K. Sharma, R.A. Yngard, Y. Lin, *Adv Colloid Interface Sci.*, **145**, 83 (2009).
23. A. Henglein, *J. Phys. Chem.*, **97**, 5457 (1993).
24. S.W. Heinzman, B. Gamem, *J. Am. Chem. Soc.*, **104**, 6801(1982).
25. Y. Tan, Y. Li, D. Zhu, *J. Colloid Interface Sci.*, **258**, 244 (2003).
26. H.A. Ewais, I.M. Ismail, K.H. Al-Fahmai, *Res. J. Chem. Environ.*, **91**, 35 (20155).
27. Z.Y. Huang, G. Mills, B. Hajek, *J. Phys. Chem.*, **97**, 11542 (1993).
28. S. K Bajpai, M. Y. Murali, M. Bajpai, R. Tankhiwale, V. Thomas, *J. Nanosci. and Nanotechnol.*, **7**, 2994 (2007).
29. Z. H. Dhoondia1, H. Chakraborty, *Nanomater. and Nanotechnol.*, **2**, 15 (2012).
30. Z. Khan, P. Kumar, Kabir-ud-Din, *J. Colloid Interface Sci.*, **290**, 184 (2005).
31. C. O. Rangel-Yagui, A. P. Junior, L. C. Tavares, *J. Pharm. Pharmaceut. Sci.*, **8**, 147 (2005).
32. C.A. Bunton, *J. Mol. Liq.*, **72**, 231 (1997).
33. M.J. Weaver, E.L. Yee, *Inorg. Chem.*, **19**, 1936 (1980)

КИНЕТИЧНИ ИЗСЛЕДВАНИЯ ПО ОБРАЗУВАНЕТО НА СРЕБЪРНИ НАНО-ЧАСТИЦИ ЧРЕЗ РЕДУКЦИЯ НА СРЕБРО (I) С ГЛЮКОЗА ВЪВ ВОДНИ И МИЦЕЛАРНИ СРЕДИ

Х.А. Еуаис^{1*}, И.М. Исмаил^{1,2}, К.Х. Ал-Фахами¹

¹Химически департамент, Научен факултет, Университет „Крал Абдул Азис“, Джеда 21413, Саудитска Арабия

²Център за върхови постижения по опазване на околната среда, Университет „Крал Абдул Азис“, Джеда 21413, Саудитска Арабия

Получена на 7 януари 2016 г.; коригирана на 14 април 2017 г.

(Резюме)

Кинетиката на образуване на сребърни нано-частици (AgNPs) чрез редукция на сребро(I) с глюкоза е изследвана при различни температури във водна мицеларна среда. Реакцията е от псевдо-първи порядък при десетократен излишък на глюкозата. Изследван е ефектът на концентрациите на натриевата основа, Ag⁺, глюкозата и цетил-триметил-амониев бромид [СТАВ]. Реакцията се ускорява при повишаване концентрацията на ОН⁻. СТАВ стабилизира растежа на наночастиците, като скоростта на реакцията се повишава с температурата. Наблюдавано е че наночастиците са сферични, агрегирани и полидисперсни. На базата на кинетичните данни е предложен и обсъден подходящ механизъм за формирането на сребърен зол. Размерите на сребърните частици са охарактеризирани чрез трансмисионна електронна микроскопия (ТЕМ) и други физико-химични и спектроскопски средства.